

Swatirupa Pani, Nilima Dash, B.K. Mohapatra\* and S.K. Singh

# Siliceous Manganese Ore from Eastern India: A Potential Resource for Ferrosilicon-Manganese Production

<https://doi.org/10.1515/htmp-2018-0081>

Received May 11, 2018; accepted October 02, 2018

**Abstract:** Siliceous manganese ore, associated with the banded iron formation occurs in large volume in northern Odisha, India. It is a sub-grade ore containing 21% Mn, 60% SiO<sub>2</sub> and 3% Fe, hence do not find any use and considered as waste. Such ore does not respond to any physical beneficiation techniques because of intricate microstructure and poor liberation of Mn-phase. It could only be up-graded to 32% Mn with 36% yield and 52% recovery by processing it through mineral separator followed by WHIMS. Siliceous manganese ore along with calcite and coke in appropriate ratio, when charged to a plasma reactor, a product with slag metal ratio of 2.5:1 was obtained within a period of 10 min. Electron probe micro-analysis of the metal confirmed it to be ferrosilicomanganese while the slag constitute of tricalcium silicate (C3S) with around 5% Mn in adsorbed state.

**Keywords:** manganese ore, Silicomanganese, Beneficiation, plasma smelting

## Introduction

Silicomanganese is widely used as a complex reducer and an alloying addition in the production of various grades of steel due to its economic and metallurgical advantages. Using SiMn instead of ferrosilicon (FeSi) and ferromanganese (FeMn) results in both reduction in production cost and technical advantages. It is also used as a semi-product in the manufacture of medium- and low-carbon ferromanganese and metallic manganese. Earlier workers [1–7] have used different raw materials like Fe-Mn slag, manganese ore, quartzite/quartz, coke/coal/charcoal as reluctant and smelted in different types

of furnaces such as: AC submerged arc furnace, ferroalloy furnace to obtain silicomanganese alloys and reported different parameters controlling its production.

Yoshikoshi et al. (1984) [1] used composite cold pellet constituting of Mn-ore, Fe-ore, fine coke and ferromanganese slag based on different charging ratio for silico-manganese production in electric furnace. Bezemer (1995) [2] while describing the silicomanganese production at Transalloys, Witbank, South Africa reported the charge mix to have manganese ore, quartzite, serpentine and coke/coal. He observed that manganese loses to slag decreased at higher basicity labels. Ding and Olsen (2000) [8] investigated the equilibrium distribution of manganese and silicon between slag and metal in silicomanganese production. They also reported an increase in silicon content with the temperature and silica content. Eissa et al. (2004) [9] reported the factors affecting silicomanganese production using Mn-rich slag in the charge. Olsen and Tangstad (2004) [3] used Mn-ore and Mn-rich slag in a electric submerged arc furnace for the production of silicomanganese. However, they indicated that high volume of slag at expense of Mn-ore will lead to larger slag/metal ratio and an increase consumption of energy in the SiMn process. While optimising Si-Mn production at Transalloys. Bisaka et al. (2004) [4] indicated that slag to metal ratio could be decreased by more than 30% by introducing high-grade Mn-ore. Different people have studied on the different reductant for the production of silicomanganese. Monsen et al. (2004) [5] mentioned about the use of charcoal as reduction material in place of coke and coal in silicomanganese production. The process of silicomanganese needs a higher temperature compared to the smelting of ferromanganese. The higher temperature is needed for successful reduction of silicon. Bench scale studies undertaken by Alex et al. (2006) [10] indicates the possibility of producing ferrosilicomanganese of the grade required by the steel industry, by reduction smelting of the residue, generated from polymetallic sea nodule after metal recovery, blended with ferromanganese slag. Eli Ringdalen et al. (2010) [11] discussed the properties Mn-ore, Mn-sinters, high carbon ferromanganese (HC Fe-Mn) slag (mixed with dolomite or calcite, quartz) and their change during silicomanganese

\*Corresponding author: B.K. Mohapatra, CSIR-IMMT, Bhubaneswar, India, E-mail: bk\_mohapatra@yahoo.com

Swatirupa Pani, Academy of scientific and Innovative Research, New Delhi, India, E-mail: swatigeol88@gmail.com

Nilima Dash: E-mail: ms.nilima@gmail.com, S.K. Singh:  
E-mail: sarojksingh@gmail.com, CSIR-IMMT, Bhubaneswar, India

production. These materials have different melting properties, which have a strong effect on reduction and smelting reactions in the production of a silicomanganese alloy. Ahmed et al. (2014) [7] used Egyptian Mn-ores mixed with ferromanganese slag to produce SiMn alloy in a submerged arc furnace at a relatively low temperature. The leached manganese nodules residue, generated by reductive roasting ammoniacal leaching of manganese nodule, blended with terrestrial Mn-ore, for production of standard grade silicomanganese (Si16Mn63), via carbothermic reduction smelting in electric arc furnace is reported by Randhawa et al. (2013) [12].

The present paper describes a different raw material i.e. naturally occurring siliceous manganese ore, that did not respond to physical beneficiation, was processed in a plasma reactor for the production of silicomanganese.

## Materials and methods

Siliceous Mn-ore samples were collected from Sankar Pit and subjected to different characterization tests prior to studying their amenability towards beneficiation such as wet high intensity magnetic separator (WHIMS), dry magnetic separator (Permaroll) and mineral separator. The bulk sample was characterised by XRD, XRF and EPMA study.

Representative Mn-ore samples were along with calcite and coke in appropriate ratio was ground and small globules were prepared by adding dextrin and processed in a plasma reactor at a temperature of approximately 1500 °C with an argon atmosphere to obtain silico-manganese metal within a short time period. This processed product was characterized by several techniques such as XRD and EPMA analysis to find out its structure and composition.

The XRD was carried out by means of Philips Diffractometer (PW-1710) having automatic divergence slit, receiving slit and graphite monochromator assembly. Cu K $\alpha$  radiation operating at 40 kV and 20 nA was used for this purpose. Each mineral phase exhibits a characteristic reflection peak of its d-values. This set of d-values was matched with JCPDS data book (1980) and various minerals were identified. Composition of siliceous manganese ore samples were analysed by XRF Spectrometry on Phillips (PW-1400) X Ray Spectrometer with Scandium and Rhodium targets using Pentaerythritol (Al, Si), Thallium Acid Pathalate (Na, Mg), Germanium (P) and Lithium Fluoride (LiF, for heavier elements) as analysing crystals in vacuum medium.

Electron probe micro analysis of bulk and processed product were done using a JEOL super probe (JXA-8200) at IMMT, Bhubaneswar. The working voltage is kept at 20 Kv with beam current as 40-100 nA. Area scanning mode is used for qualitative analysis and X-ray scanning to find out elemental distribution.

## Results and discussion

### Characterisation

#### Mineralogical characteristics

The siliceous Mn-ore appears either as hard-laminated (Figure 1(a)) or hard-mosaic (Figure 1(c)). The former type is indistinctly laminated with alternate quartz and manganese lamina and traversed by thin secondary manganese veins. Under optical microscope fine grained quartz is found intimately associated with fine grained cryptomelane (Figure 1(b)). In hard-mosaic type, elongated fragments of quartz are seen enclosed within manganese.

Under microscope, quartz in different shape and size are seen embedded within cryptomelane/romanechite (Figure 1(d)). XRD pattern of the siliceous Mn-ore (Figure 2), shows the presence of quartz, cryptomelane and pyrolusite.

#### Chemical characteristics

The bulk samples of Shankar deposit contain 22% Mn and 59.60% silica with minor iron (Table 1). High silica is mostly attributed to quartz, while Mn content is contributed by pyrolusite, cryptomelane/romanechite. Iron occurs as minor constituent which is mainly attributed to hematite. X-Ray image map under electron microprobe (EPMA), illustrated in Figure 3, shows intimate association of silica and manganese.

### Beneficiation

To assess the response to up-gradation, the low-grade siliceous Mn-ore was processed through various beneficiation techniques such as: size classification, heavy media separation, mineral separator and dry and wet high intensity magnetic separator (WHIMS).

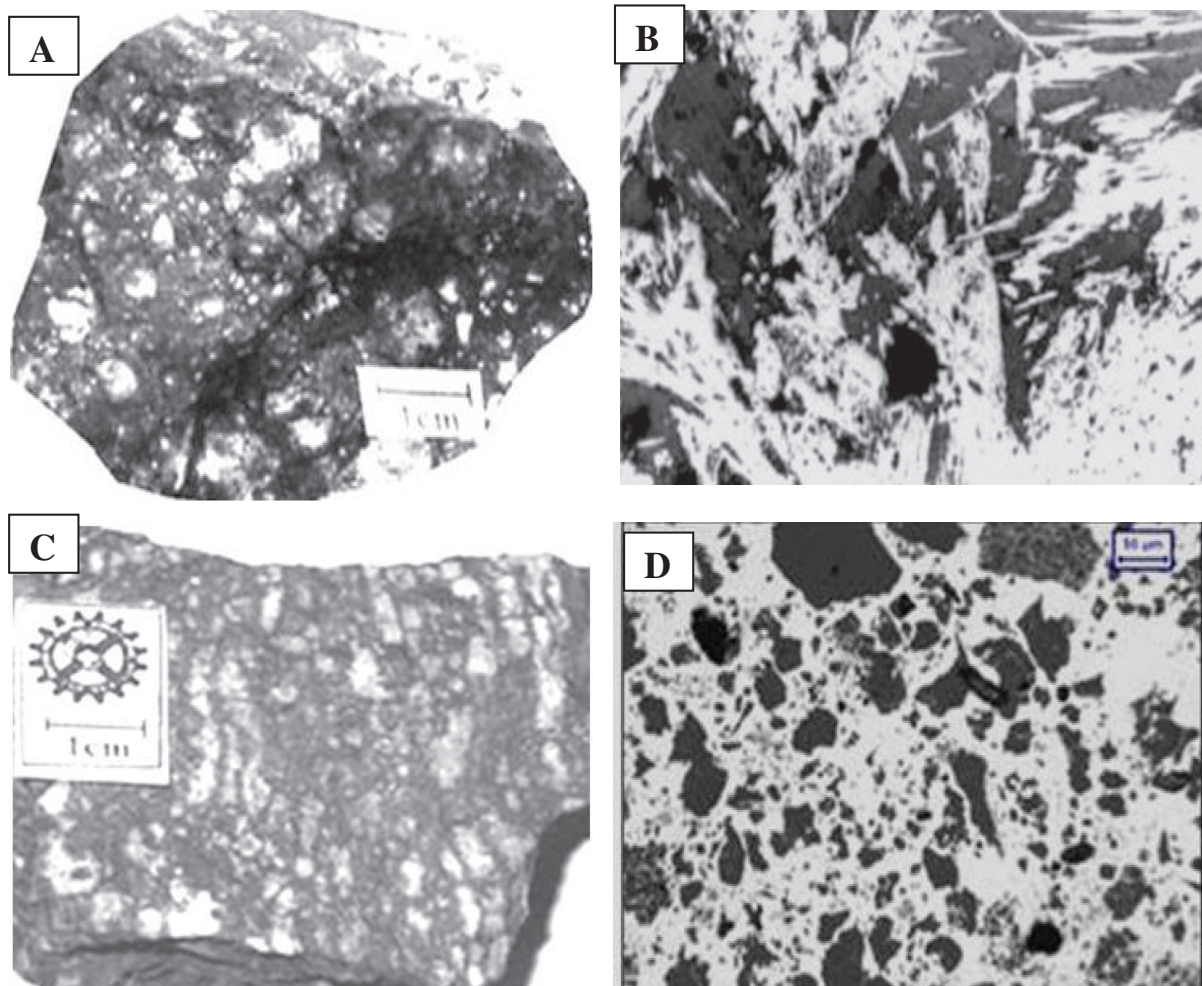


**Figure 1:** Visual Image (A & C) and photomicrograph (B & D) of siliceous manganese ore. (A). Hard and compact siliceous Mn-ore, containing irregular clots of quartz. (B). Fine grained quartz (black) occupying the inter-granular space pyrolusite (white) (Scale as that of D), (C). Siliceous Mn-ore showing massive-mosaic texture, (D). Quartz in different shape and size (black) embedded within cryptomelane/romanechite.

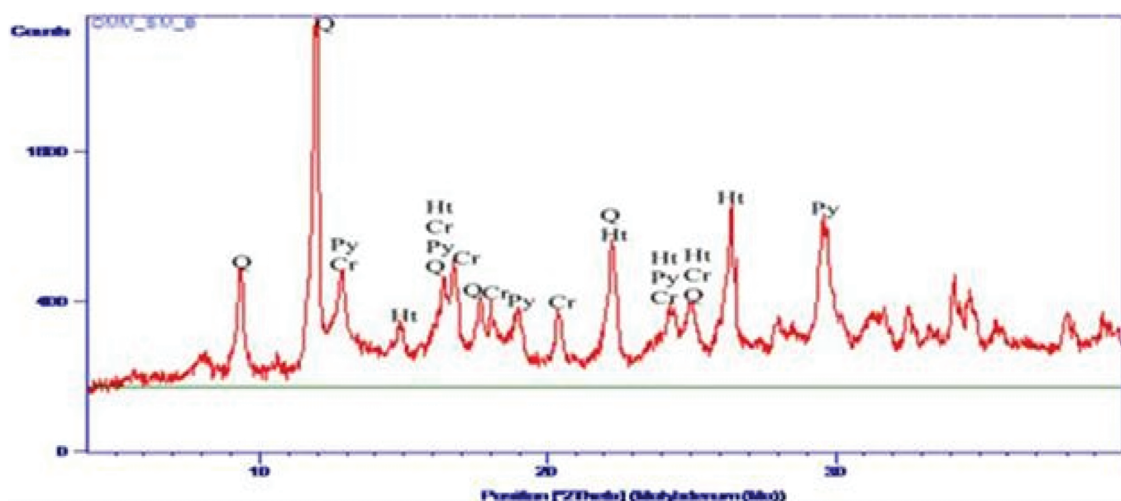


**Figure 2:** X-ray diffraction pattern of Siliceous Mn-ore [Py-Pyrolusite; Cr- Cryptomelane; Q- Quartz; Ht- Hematite].

**Table 1:** Partial chemical analysis of feed siliceous Mn-ore.

Mn%	SiO <sub>2</sub> %	Fe%
21.93	59.60	3.12

### Size classification

The bulk sample was ground to below 1 mm through jaw crusher followed by roll crusher and separated into two size fractions such as  $-1\text{ mm} + 0.1\text{ mm}$  and  $-0.1\text{ mm}$ . Both the fractions were analysed for Mn and SiO<sub>2</sub> content (Table 2). Relatively higher manganese value is seen in the coarser fraction.

### Heavy media separation

The  $-1\text{ mm} + 0.1\text{ mm}$  fraction from the low-grade Mn-ore was subjected to sink and float studies using

bromoform as the separating medium. The results of the studies are presented in Table 3. From the sink and float studies, it can be inferred that gravity method of physical separation would not respond well to beneficiation. Thus, if siliceous Mn-ore from Shankar deposit is subjected to heavy media separation, only 61% of it could be upgraded to a product containing only 28.47% Mn.

### Magnetic separation

The coarse classified fraction ( $-1 + 0.1\text{ mm}$ ) was subjected to dry magnetic separation (Permaroll) at 1.00 tesla. The finer fraction ( $-0.1\text{ mm}$ ) was subjected to wet high intensity magnetic separation (SALA). It is observed that the magnetic product obtained through dry separation showed better result than in wet separation. However, the feed of 22% Mn can be upgraded to only 26% Mn with 40% yield. The comparative results of both dry and wet separation are given in Table 4.

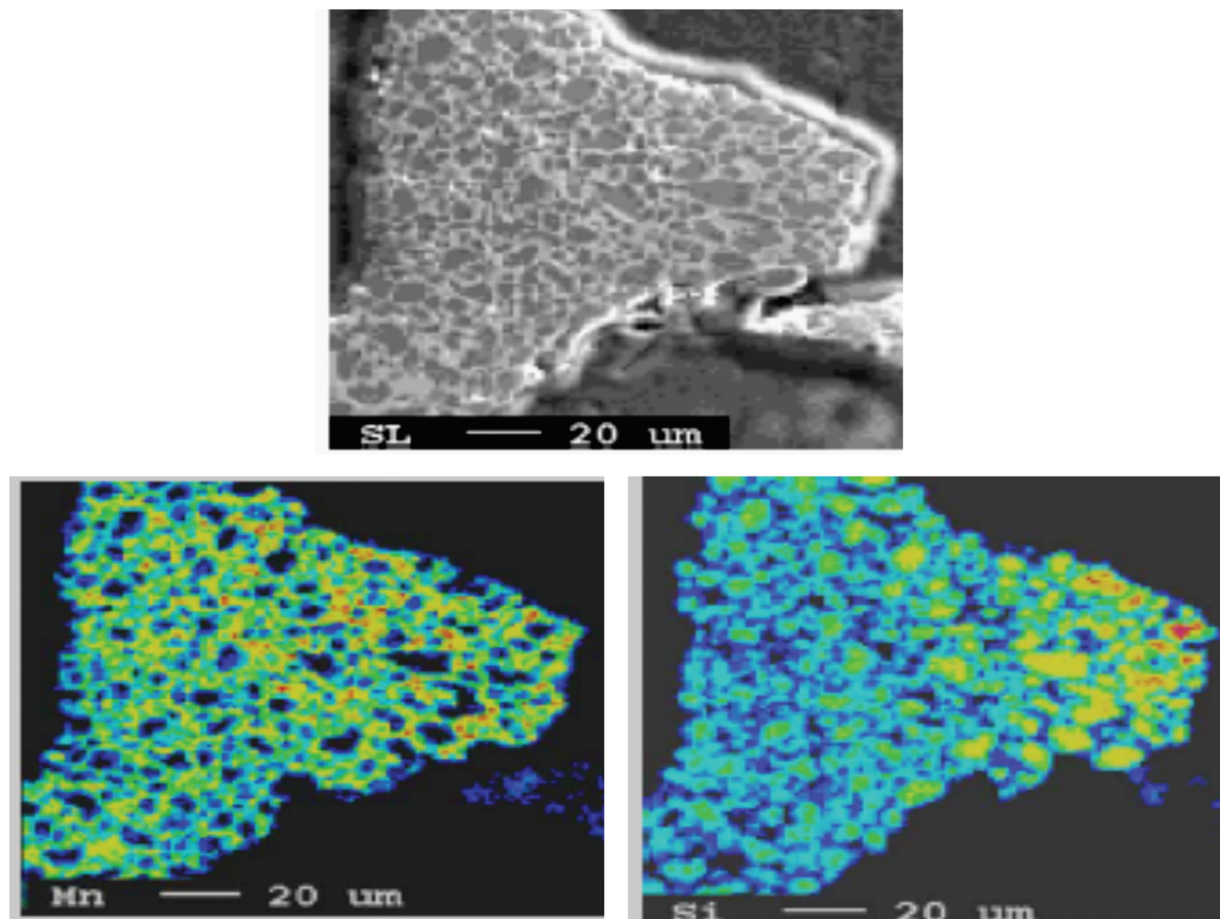


**Figure 3:** Compositional map showing distribution pattern of Mn and Si in a typical siliceous Mn-ore, exhibiting mosaic texture under EPMA.

**Table 2:** Partial chemical analysis of sieve fractions of siliceous Mn-ore.

Size, in mm	Weight%	Mn%	SiO <sub>2</sub> %
-1 + 0.1	92.03	21.55	60.17
-0.1	7.97	17.74	47.70
Head	100	21.25	59.60

**Table 3:** Results of Sink and float studies of siliceous Mn-ore.

	-1 + 0.1 mm		-0.1 mm
	Sink	Float	Not treated
Weight%	61.28	30.75	7.97
Mn%	28.47	7.30	17.74

**Table 4:** Results of magnetic separation processed through Dry Magnetic Separator (DMS) and Wet High Intensity Magnetic Separator (WHIMS).

Size in mm	Medium	Nature	Wt% w. r.t feed	Mn%
-1 + 0.1	Dry [Permaroll]	Magnetic	39.39	26.27
		Non-magnetic	52.64	17.42
-0.1	Wet [WHIMS]	Magnetic	5.12	21.27
		Non-magnetic	2.85	11.42

### Processing through mineral separator followed by WHIMS

Considering better liberation of manganese phases at coarser size, the -1 + 0.1 mm fraction was ground below 0.1 mm by roll crusher and processed through a mineral separator. Results are shown in Table 5. The mineral separator concentrate was then processed through WHIMS and results are shown in Table 6.

**Table 5:** Results of mineral separator (Size: -0.1 mm).

Size in mm	Sample details	Wt%	Mn%	SiO <sub>2</sub> %
-0.1	Concentrate	50.50	28.91	37.53
	Tailing	49.50	15.84	82.11

The conceptual flow sheet comparing the extent of beneficiation of sub-grade siliceous manganese ore from Shankar is shown in Figure 4.

**Table 6:** Concentrate of Mineral Separator subjected to WHIMS.

Mag/Nmag	Weight%	Weight% wrt feed	Mn%	SiO <sub>2</sub> %
Mag	60.00	35.83	31.8	26.45
Non-mag	40.00	14.67	21.85	64.58

### Inference on physical beneficiation of siliceous Mn-ore

The sub-grade siliceous Mn-ore could only be upgraded to a low-grade Mn-ore by adopting physical beneficiation technique. A feed of 21.93% Mn was upgraded to 31.80% Mn with 35.83% yield and 52% recovery. In this process though silica content could be reduced, around 26.45% SiO<sub>2</sub> still remains in the product. Further, around 64 volume % of the ore goes as reject after beneficiation, which contains appreciable amount of Mn (~16%). Hence, this physical beneficiation process was not considered cost effective. As an alternative, to recover the metal values from the siliceous Mn-ore, it was subjected to smelting studies.

### Smelting

The smelting study was carried out in a plasma reactor as a small scale experiment with the following charge mix (Table 7). The average run time is about 10 min. This charge mix, in form of small granules, was processed through a plasma reactor at a temperature of approximately 1500 °C with an argon atmosphere. Within a very short period two distinctly separated phases were obtained with slag metal ratio of 2.5:1.

### Characterisation of metal

The density of the metal [Ferro silico manganese alloy] was determined to be 5.56. The XRD pattern of the metal shows single SiMn phase (Figure 5). The XRD peaks diagnostic of silicomanganese metal are: 2.03 Å (100), 1.85 Å (48) and 1.37 Å (8). The electron micrographs of metal [both SEI and compo image] are shown in Figure 6. The X-Ray image map of the metal shows two prominent phases: one bright nodular and the other grey matrix (Figure 7). The *in-situ* EDAX analysis of these two phases taken under an electron microprobe is shown in Table 8. From the analysis results the metal is identified as ferro-silico manganese alloy.

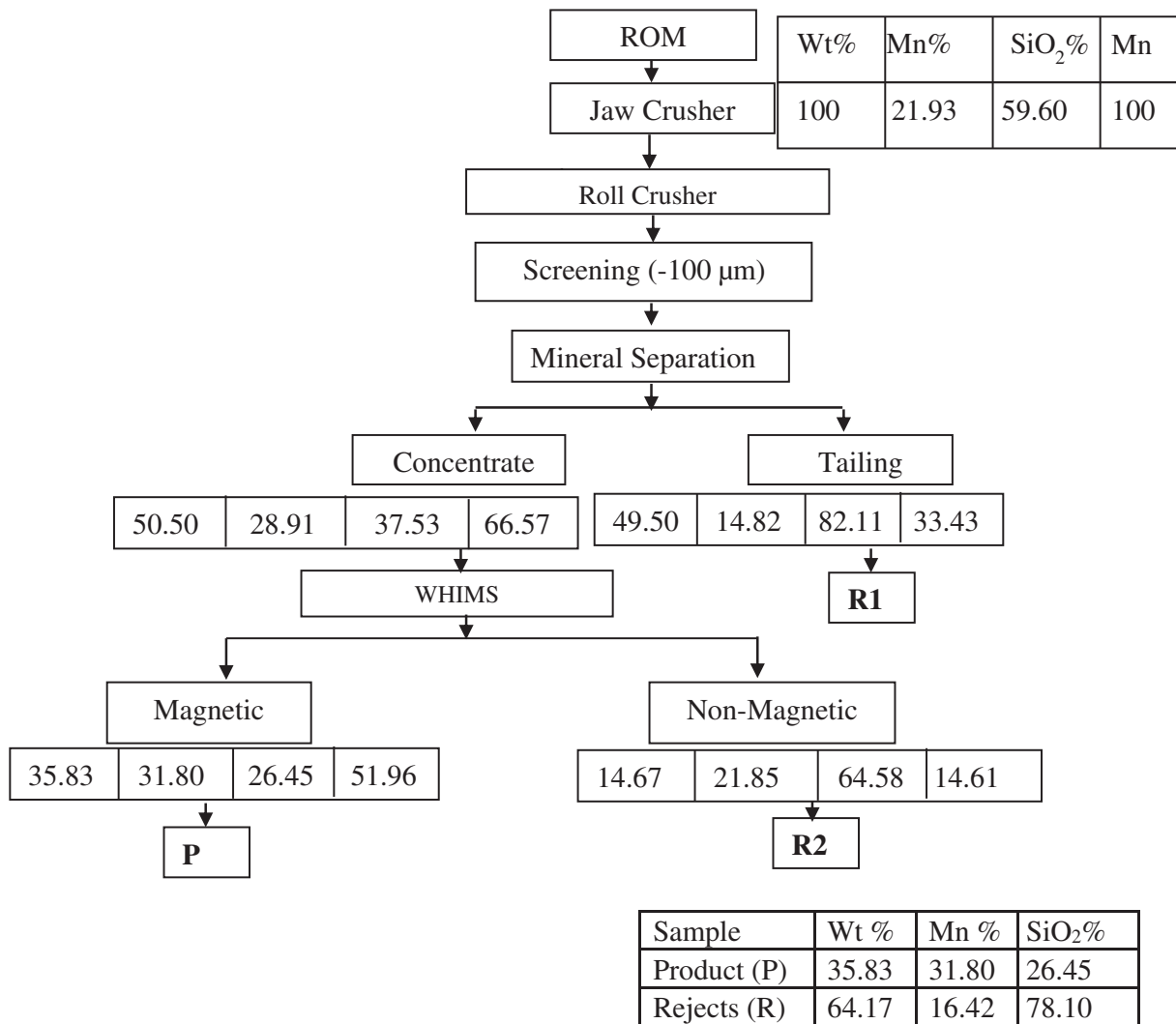


**Figure 4:** Conceptual flow sheet showing beneficiation steps of siliceous Mn-ore.

**Table 7:** Details of charge mix in the feed.

Charge mix	Wt., in gm
Siliceous Mn-ore	200
Coke	50
Calcite	80
Dextrin	15

The EPMA results of both the phases exhibit similar Mn content, but the bright phase show higher iron and lower silicon values than the grey phase. A line scan (along X-Y) showing the distribution of Si, Mn and Fe on a magnified view of the metal comprising both bright and grey phase is shown in Figure 8. As can be seen from the electron micrograph, though no distinct compositional

difference between the two phases is seen, very high Mn counts are recorded as compared to Si.

#### Characterisation of slag

The slag obtained from plasma reactor was examined under electron microprobe. The electron micrograph (compo image) of the sample (Figure 9) shows two phases: greyish white and greyish dark. A few micron size metallic prills (white) are also noticed. The EDS patterns of these two phases are shown in Figures 10 & 11. As can be seen from the spectra both the phases are composed of tricalcium silicate ( $C_3S$ ). Though the slag in general contains minor amount Mn (~5%), its relative abundance is seen in greyish white phase. Trace of alumina is observed in

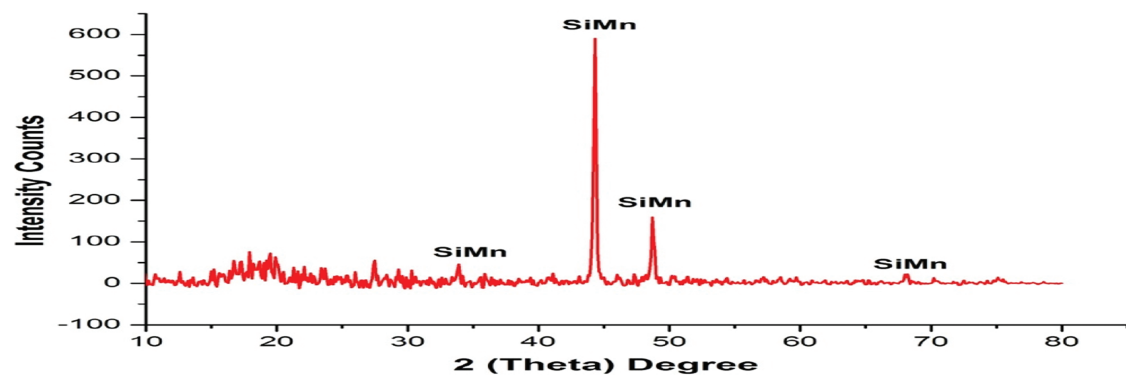


Figure 5: XRD pattern of Silico-manganese alloy.

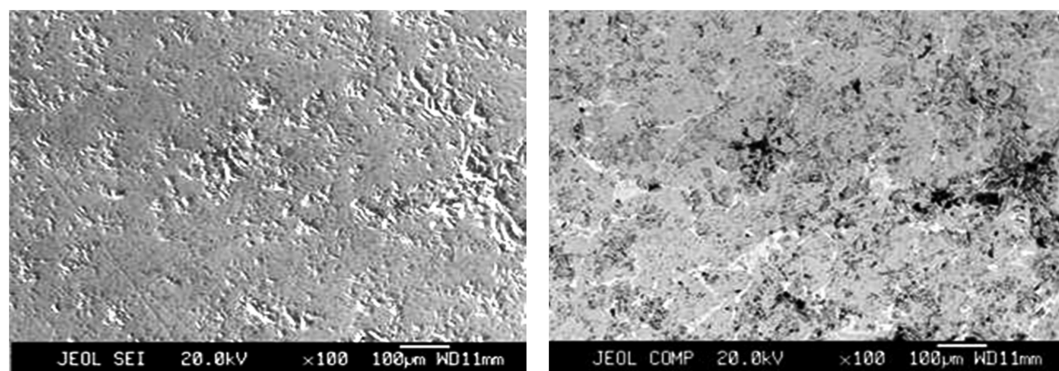


Figure 6: Electron micrographs [SEI & Compo] of Si-Mn alloy.

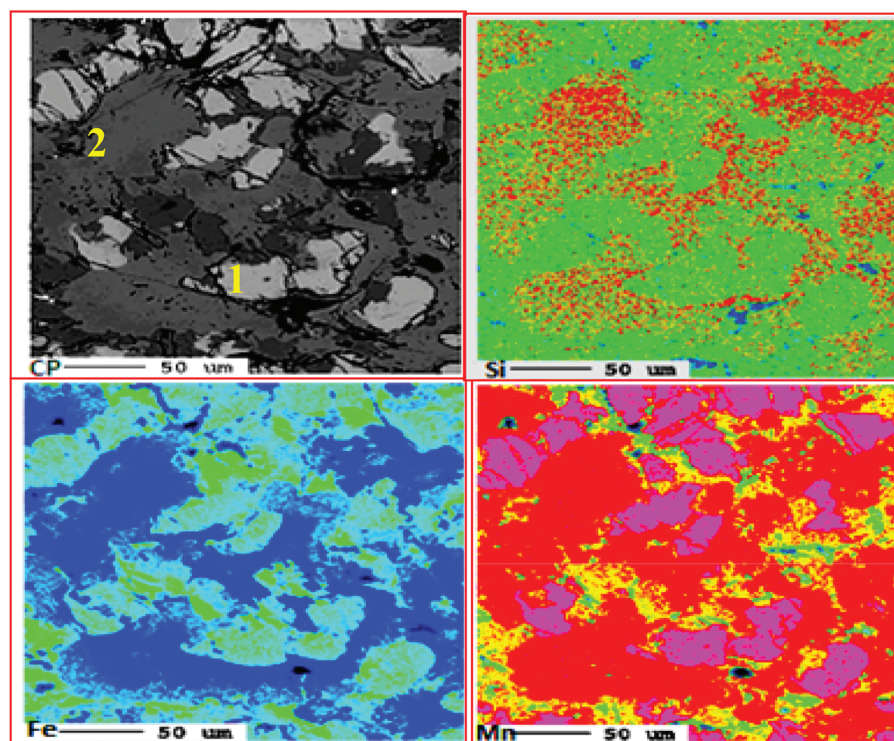
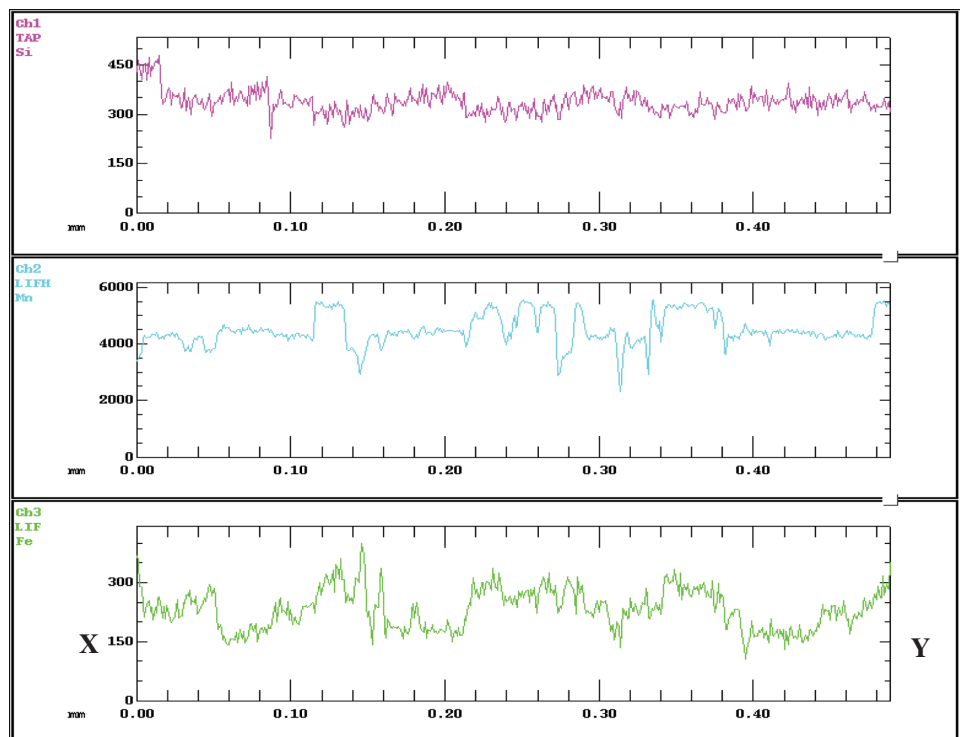
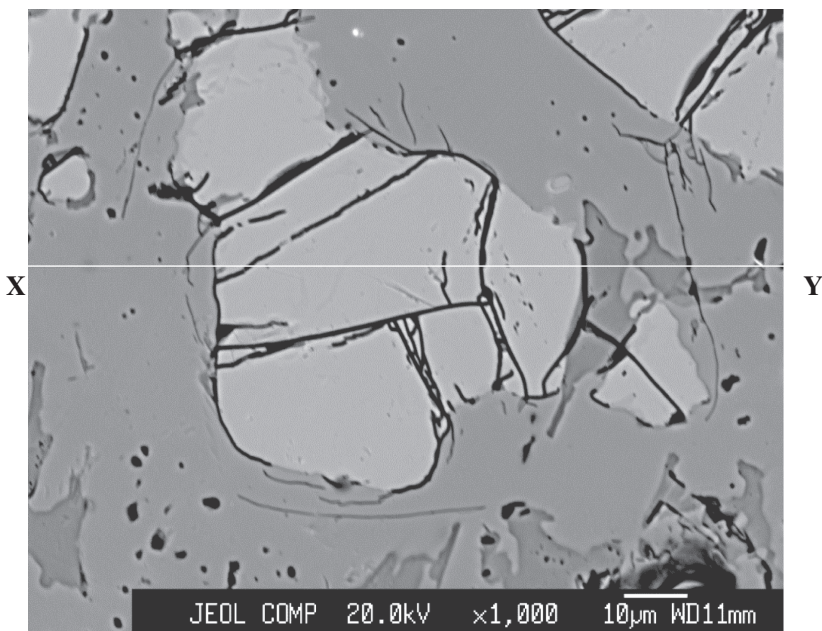


Figure 7: Distribution of Si, Fe, Mn in silico-manganese alloy.

**Table 8:** EPMA results of silico-manganese alloy.

Wt%	White phase (1)	Gary phase (2)
Si	29.52	32.78
Fe	9.98	7.05
Mn	60.50	60.17
Total	100	100

**Figure 8:** Element distribution spectra along X-Y line shown in the above figure.

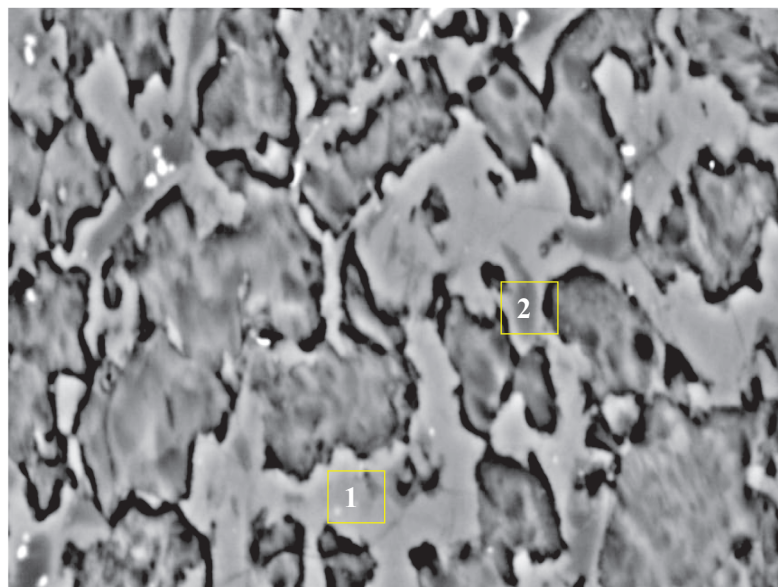


Figure 9: Electron micrograph of Si-Mn slag. 1 and 2- EDS point.

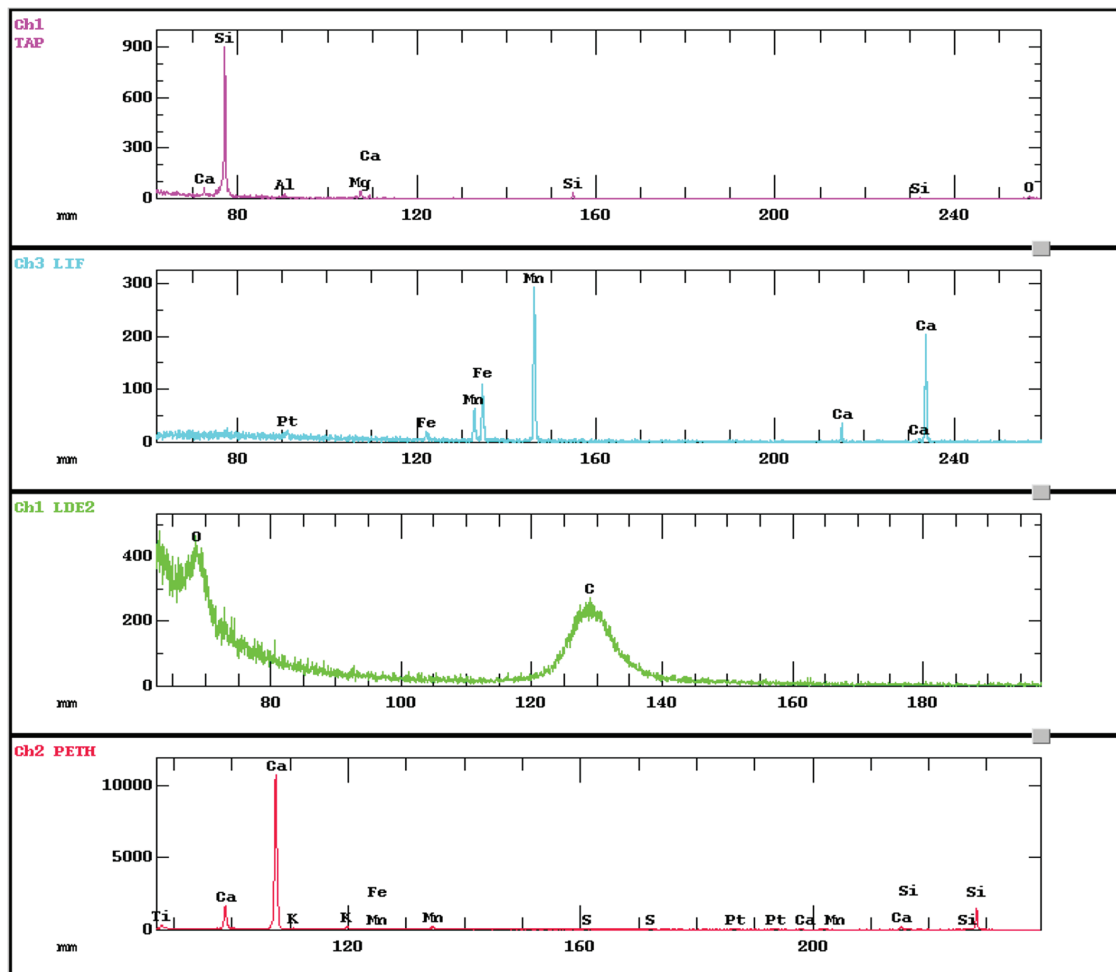


Figure 10: EDS pattern of *in-situ* analysis at point 1 shown in Figure 9.

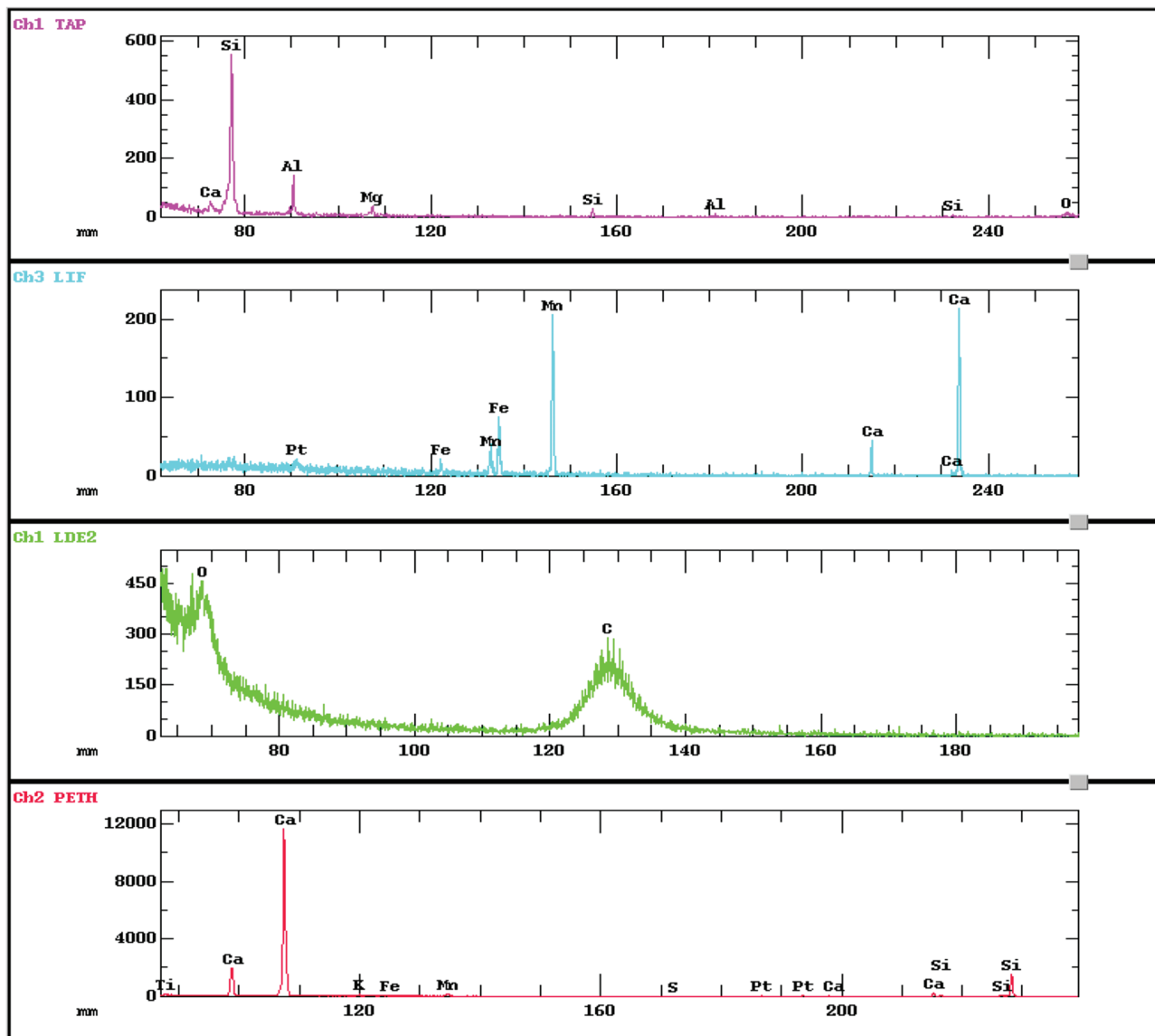


Figure 11: EDS pattern of *in-situ* analysis at point 2 shown in Figure 9.

greyish dark phase. Presence of carbon is also recorded in the slag.

## Conclusions

From the foregoing discussion, the following conclusions are made:

1. Siliceous manganese ore, available in large volume in Odisha, contains only 21% of Mn and hence do not find use in ferroalloy industry.
2. Such ore do not respond to physical beneficiation for its intricate microstructure and poor liberation of Mn-phases.
3. When this ore is processed in plasma reactor, ferro-silicon-manganese alloy was produced (having slag metal ratio of 2.5:1) within a period of 10 min.

4. The ferrosilicon-manganese alloy constituting of 29–33% Si, 60% Mn and 7–10% Fe can be used as a complex reducer and an alloying addition in the production of various grades of steel due to its economic and metallurgical advantages. It can also be used in the manufacture of medium and low carbon ferromanganese and metallic manganese.
5. Manganese and silicon are crucial constituents in steel making, as deoxidants, desulphurizers. The ferrosilicon-manganese alloy can be used as a substitute of two individual raw materials for economic reasons.
6. The slag, rich in C3S can be used as a raw material in cement industry.
7. In view of use of such alloy in steel making, the present work on preparation of ferrosilico manganese alloy from a low cost material [naturally occurring siliceous manganese ore] through pyrometallurgical route bears significance as a futuristic product.

**Acknowledgements:** The authors are grateful to Director, CSIR-Institute of Minerals and Materials Technology (IMMT), Bhubaneswar, Odisha for providing infrastructural facilities. The authors are thankful to Mrs Swagatika Mohanty of IMMT, for carrying out XRD analysis.

## References

- [1] H. Yoshikoshi, O. Takeuchi, T. Miyashita, T. Kuwana and K. Kishikawa, *Trans. ISIJ*, 24 (1984) 492–497.
- [2] K. Bezemer, The proceedings of INFACON 7, Trondheim, Norway (1995), pp. 573–580.
- [3] S.E. Olsen and M. Tangstad, Proceeding: Tenth International Ferroalloys Congress; INFACON X; 'Transformation through Technology', ISBN: 0-9584663-5-1 (2004).
- [4] K. Bisaka, J. Griesel and P.H.F. Bouwer, Proceedings: Tenth International Ferroalloys Congress; INFACON X; 'Transformation through Technology', ISBN: 0-9584663-5-1 (2004).
- [5] B. Monsen, M. Tangstad and H. Midtgård, Proceeding: Tenth International Ferroalloys Congress; INFACON X; 'Transformation through Technology', ISBN: 0-9584663-5-1 (2004).
- [6] H. El-Faramawy, T. Mattar, A. Fathy, M. Eissa and A.M. Ahmed, *Ironmaking Steelmaking, Processes, Prod. Appl.*, 31 (2004) 31–36.
- [7] A. Ahmed, S. Ghali, M.K. El-Fawakhry, H. El-Faramawy and M. Eissa, *Ironmaking Steelmaking, Processes, Prod. Appl.*, 41 (2014) 310–320.
- [8] W. Ding and S.E. Olsen, *ISIJ Int.*, 40 (2000) 850–856.
- [9] M. Eissa, A. Fathy, A. Ahmed, A. El-Mohammady and K. El-Fawakhry, Proceeding: Tenth International Ferroalloys Congress; INFACON X; 'Transformation through Technology', ISBN: 0-9584663-5-1 (2004).
- [10] T. C. Alex, K. M. Godiwalla, S. Kumar, R. K. Jana, A. S. Rao, M. Singh and Premchand, *Steel. Res. Int.*, 77 (2006) 147–151.
- [11] E. Ringdalen, S. Gaal, M. Tangstad and O. Ostrovski, *Metall. Mater. Tran. B*, 41 (2010) 1220–1229.
- [12] N. S. Randhawa, R. K. Jana and N. N. Das, *Miner. Process. Extr. Metall.*, 122 (2013) 6–14.